

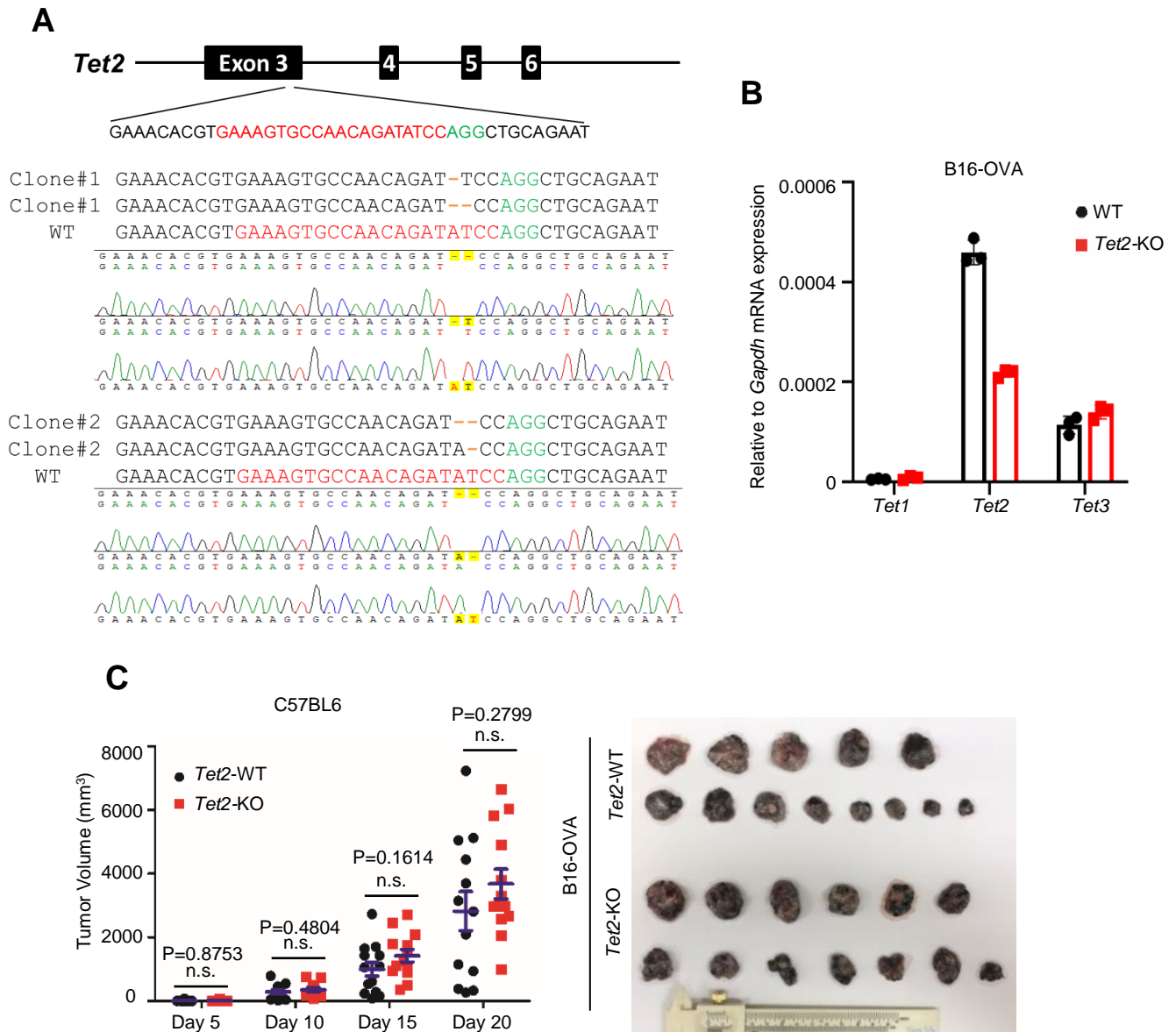
Supplemental Table 1 : Sequence for qPCR and CHIP-qPCR primers**Primers for qPCR**

Gene	Forward: Sequence (5'-3')	Reverse: Sequence (5'-3')
Human CXCL9	GTGGTGTTCCTTTCTCTTGGG	ACAGCGACCCTTTCTCACTAC
Human CXCL10	CTCCAGTCTCAGCACCATGA	GCTCCCCTCTGGTTTTAAGG
Human CXCL11	ATGCAAAGACAGCGTCCTCT	CAAACATGAGTGTGAAGGGC
Human PDL1	TGGCATTGCTGAACGCATT	TGCAGCCAGGTCTAATTGTTTT
Human GAPDH	ATGACATCAAGAAGGTGGTG	CATACCAGGAAATGAGCTTG
Mouse Cxcl9	GAGCAGTGTGGAGTTCGAGG	TCCGGATCTAGGCAGGTTTG
Mouse Cxcl10	AATGAGGGCCATAGGGAAGC	AGCCATCCACTGGGTAAAGG
Mouse Cxcl11	GCTTTCTCGATCTCTGCCAT	AACAGGAAGGTCACAGCCAT
Mouse Pdl1	GCTCAAAGGACTTGTACGTG	TGATCTGAAGGGCAGCATTTTC
Mouse Gapdh	TGGAGAAACCTGCCAAGTATGA	CTGTTGAAGTCGCAGGAGACAA
Mouse Tet1	GCAGTGAACCCCGGAAAAC	AGAGCCATTGTAAACCCGTTG
Mouse Tet2	AGAGAAGACAATCGAGAAGTCGG	CCTTCCGTACTCCCAAACATCAT
Mouse Tet3	TGCGATTGTGTCGAACAAATAGT	TCCATACCGATCCTCCATGAG
Human Tet1	CATCAGTCAAGACTTTAAGCCCT	CGGGTGGTTTAGGTTCTGTTT
Human Tet2	GATAGAACCAACCATGTTGAGGG	TGGAGCTTTGTAGCCAGAGGT
Human Tet3	GCCGGTCAATGGTGCTAGAG	CGGTTGAAGGTTTCATAGAGCC
Mouse Usp15	CGACGCTGCTCAAAACCTC	CGATGGGTCCAGGATAGACATT

Primers for CHIP-qPCR

Gene	Forward: Sequence (5'-3')	Reverse: Sequence (5'-3')
CXCL10	AACAGTTTCCGGGAAAGCATT	ATCCCGCTTTAGTTTCCGTTTC
PD-L1	AACACTAGATACCTAAACTGAAAGCTT CC	GGCCCGGAGGCGG

Supplemental Figure 1



Supplemental Figure 1: Loss of *Tet2* confers tumor resistance to immunotherapy.

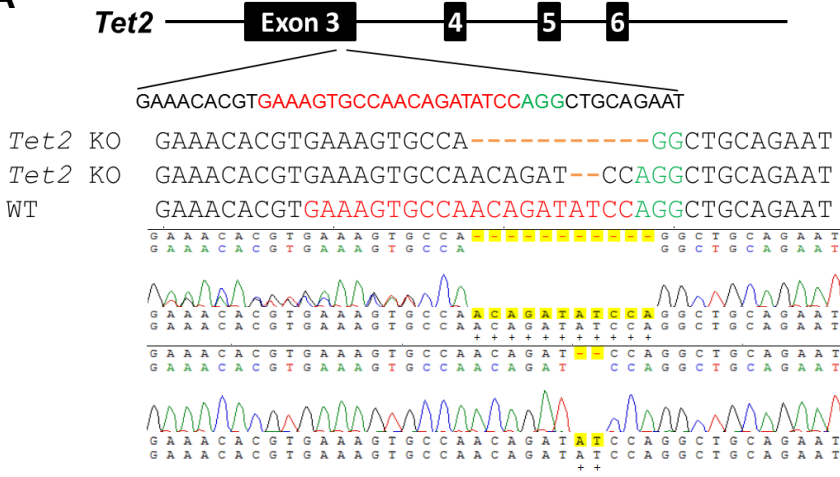
(A): Genotype of *Tet2* KO B16-OVA melanoma cells is shown. Genomic DNA of *Tet2* KO B16-OVA melanoma clones was extracted, and their genotypes were determined by PCR-sequencing. sgRNA sequence is colored as red and PAM is colored as green.

(B): *Tet1*, *Tet2* and *Tet3* gene expression in B16-OVA cells is shown. Total RNA of B16-OVA cells was extracted and mRNA levels of *Tet1*, *Tet2* and *Tet3* were determined by qPCR. Error bars represent \pm SD for triplicate experiments.

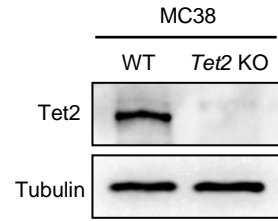
(C): *Tet2* KO B16-OVA cells derived tumor grow similarly to wild type cells in C57BL/6 mice. Tumor growth for mice injected with WT or *Tet2* KO B16-OVA cells in C57BL/6 mice was determined every five days and analyzed. Data represent mean \pm SEM for 13 tumors.

Supplemental Figure 2

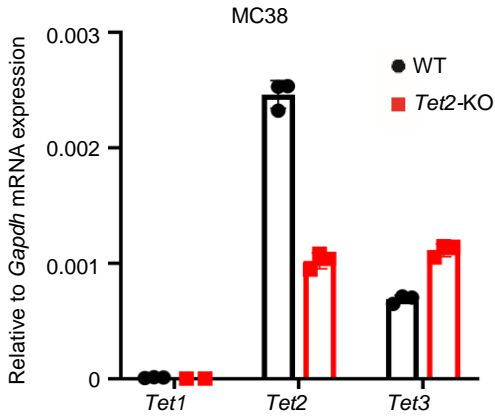
A



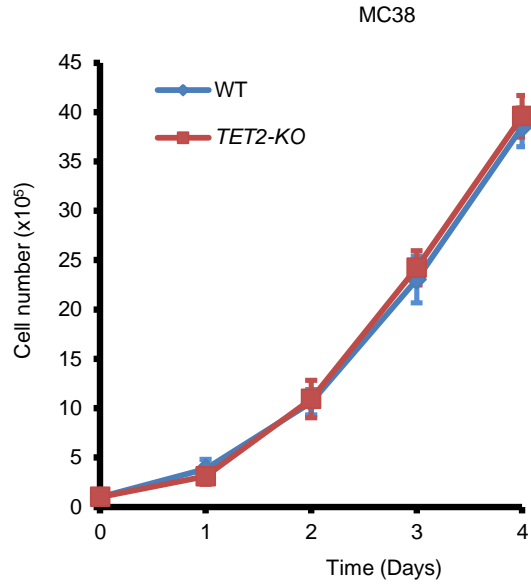
B



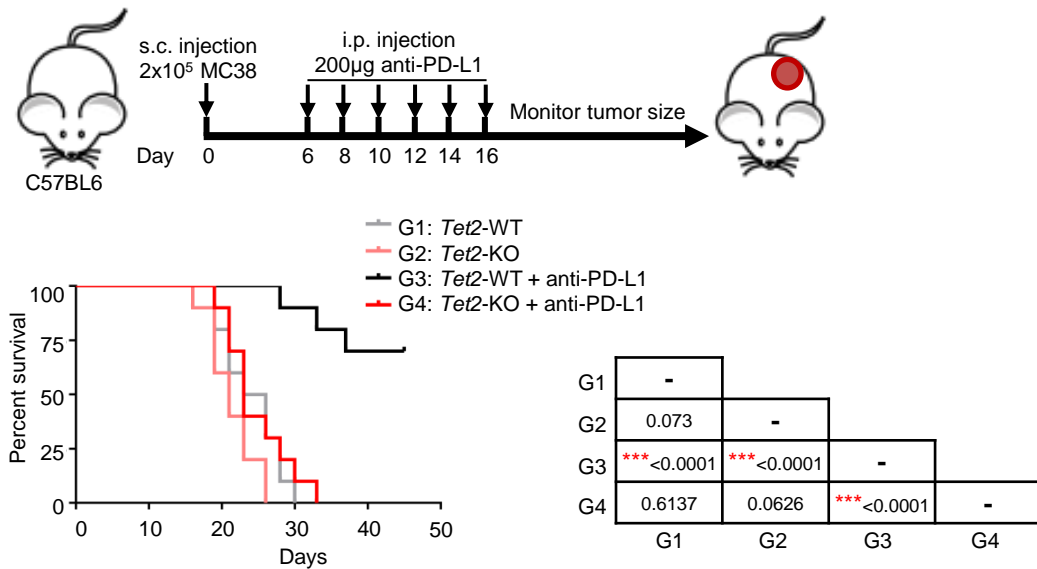
C



D



E



Supplemental Figure 2: Loss of *Tet2* confers tumor resistance to immunotherapy.

(A): Genotype of *Tet2* KO MC38 cells is shown. Genomic DNA of *Tet2* KO MC38 single cells clone was extracted, and their genotype were determined by PCR-sequencing. sgRNA sequence is colored as red and PAM is colored as green.

(B): Western-blot confirmation of *Tet2* KO in MC38 cells is shown.

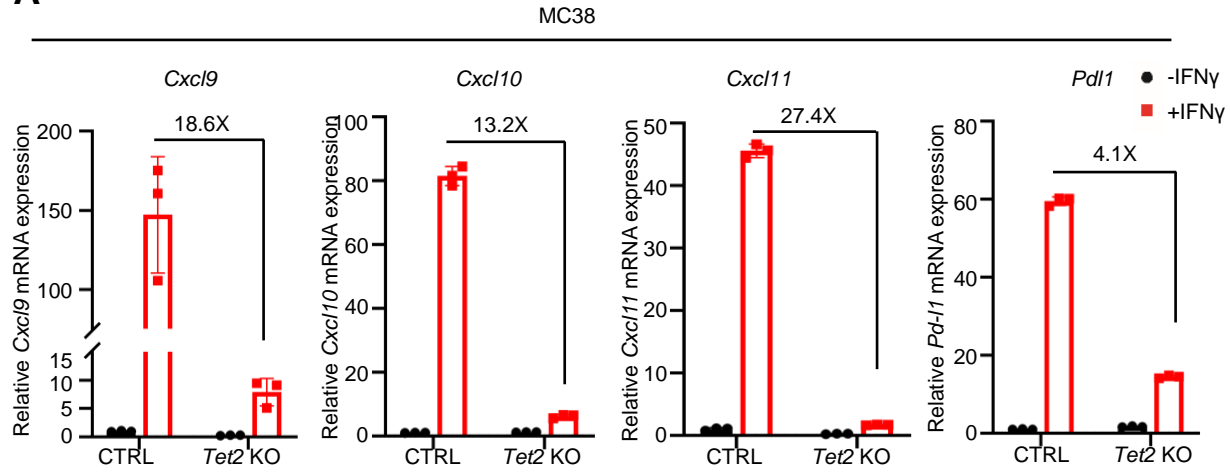
(C): *Tet1*, *Tet2* and *Tet3* gene expression in MC38 cells is shown. Total RNA of MC38 cells was extracted and mRNA levels of *Tet1*, *Tet2* and *Tet3* were determined by qPCR. Error bars represent \pm SD for triplicate experiments.

(D): *Tet2* KO MC38 cells proliferate similarly to wildtype cells in culture. Proliferation curves for *Tet2* WT and KO MC38 cells were determined by seeding same number of cells and counting every day. Error bars represent cell numbers \pm SD for triplicate experiments.

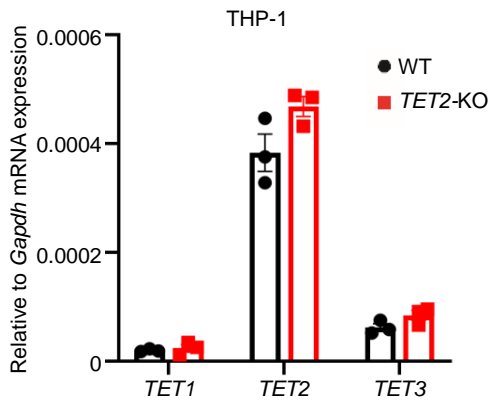
(E): Kaplan-Meier survival curves for mice injected with WT or *Tet2* KO MC38 cells and treated with anti-PD-L1 therapy are shown. 2×10^5 WT or *Tet2* KO MC38 cells and anti-PD-L1 antibody were s.c. and i.p. injected to C57BL/6 mice at indicated time points, respectively. Kaplan-Meier survival curves for these mice are shown (n = 10 mice for each group). The p value was determined using Log-rank (Mantel-Cox) test, comparing each two group, and was shown in the table of the figure, ***p < 0.001.

Supplemental Figure 3

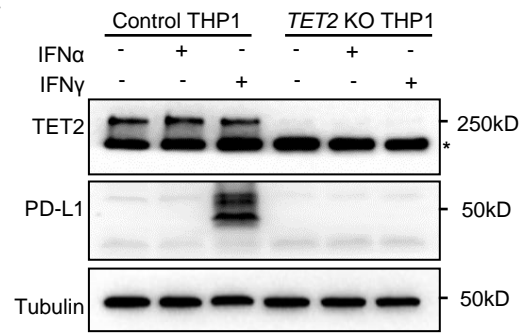
A



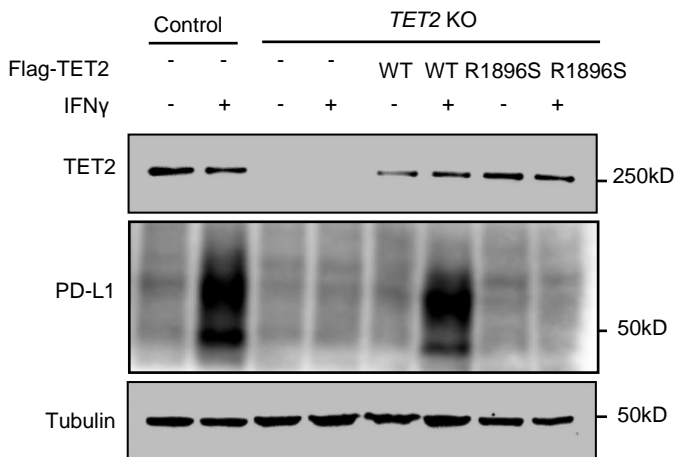
B



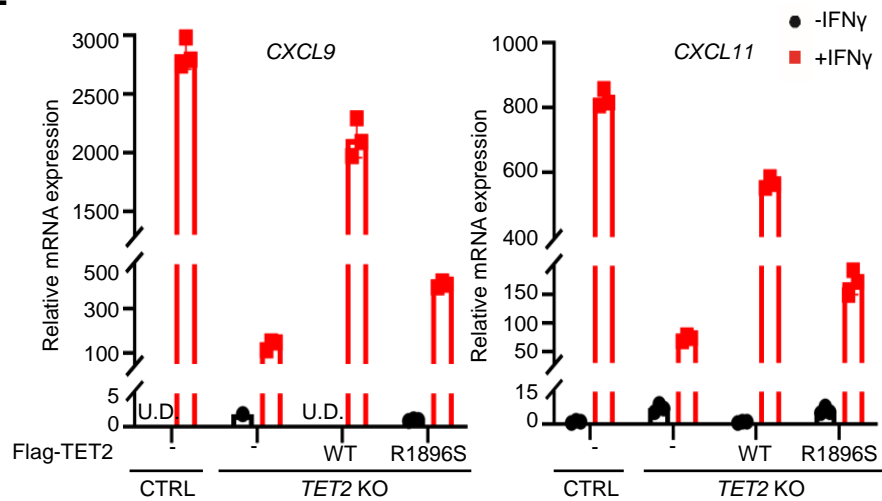
C



D



E



Supplemental Figure 3: TET2 activates T_H1-type chemokines and PD-L1 expression.

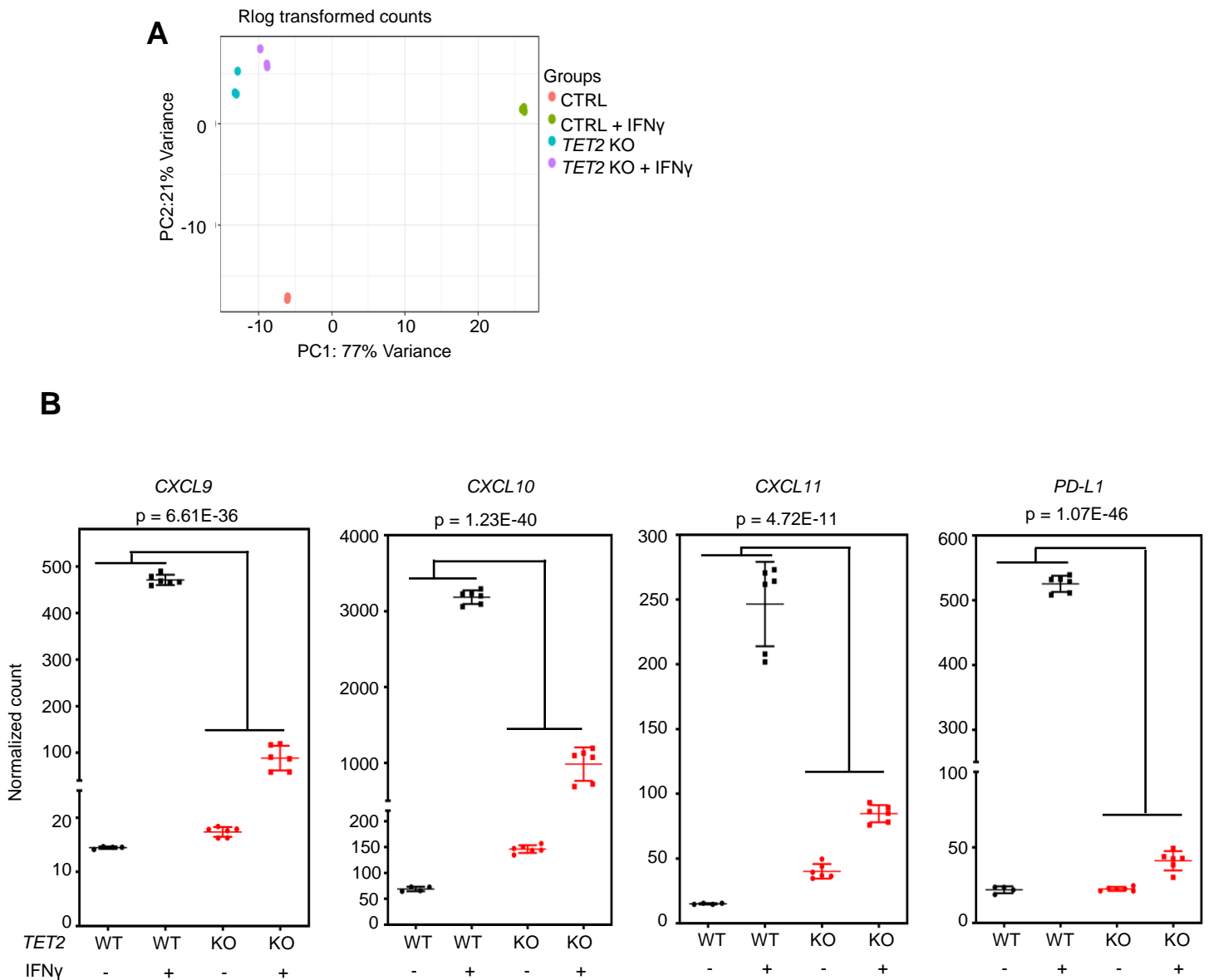
(A): Knocking out Tet2 blocks IFN γ -induced chemokines and *Pdl1* gene expression in MC38 cells. WT or *Tet2* KO MC38 cells were treated with mouse IFN γ for 20hrs and total RNA was extracted. The relative mRNA levels of chemokines and *Pdl1* were determined by qPCR. Error bars represent \pm SD for triplicate experiments.

(B): *TET1*, *TET2* and *TET3* gene expression in THP-1 cells is shown. Total RNA of THP-1 cells was extracted and mRNA levels of *TET1*, *TET2* and *TET3* were determined by qPCR. Error bars represent \pm SD for triplicate experiments.

(C): Knocking out TET2 decreased IFN γ -induced PD-L1 protein level. WT or *TET2* KO THP-1 cells were treated with IFN γ for 30hrs and protein level of PD-L1 was determined by western blot, * indicates unspecific band.

(D, E): TET2 catalytic activity is required for IFN γ induced *CXCL9*, *CXCL11* and PD-L1 expression. TET2 WT and catalytic mutant R1896S were over-expressed in *TET2* KO THP-1 cells, then cells were treated with IFN γ for 20hrs as indicated and total RNA was extracted. The TET2 expression and protein levels of PD-L1 were determined by western blot (**D**), and the relative mRNA levels of *CXCL9* and *CXCL11* were determined by qPCR (**E**), U.D. means undetectable. Error bars represent \pm SD for triplicate experiments.

Supplemental Figure 4



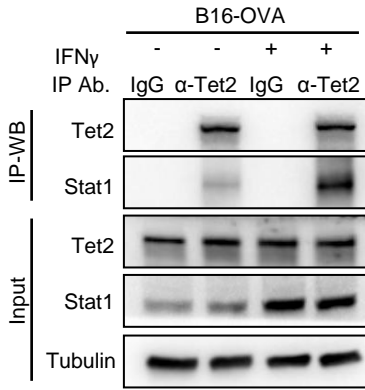
Supplemental Figure 4: Loss of TET2 alters IFN γ transcriptome

(A): Plot of principal components 1 and 2 from analysis of gene-expression levels (RNA-seq) in 11 samples. Similarities of gene expression patterns were calculated and mapped for WT and TET2 KO THP-1 cells with or without IFN γ treatment.

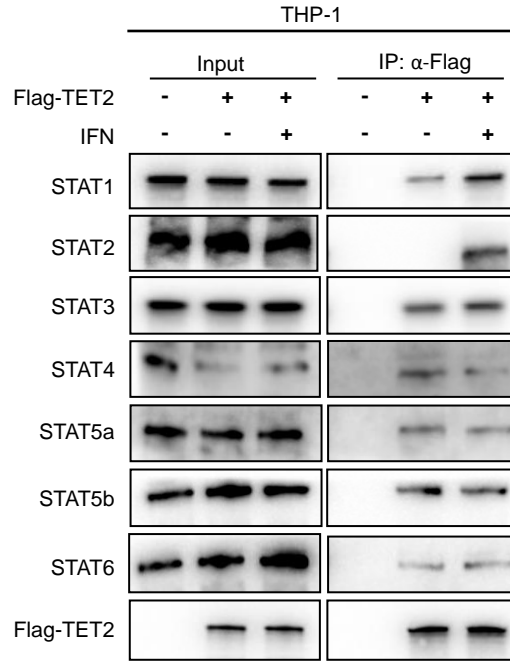
(B): Knocking out TET2 blocks IFN γ -induced CXCL9/10/11 and PD-L1 gene expression in THP-1 by RNA-Seq. WT or TET2 KO THP-1 cells were treated with IFN γ for 20hrs, total RNA was extracted and subjected for RNA-seq. Normalized counts of CXCL9/10/11 and PD-L1 from RNA-Seq were analyzed and shown. Data represent mean \pm SD.

Supplemental Figure 5

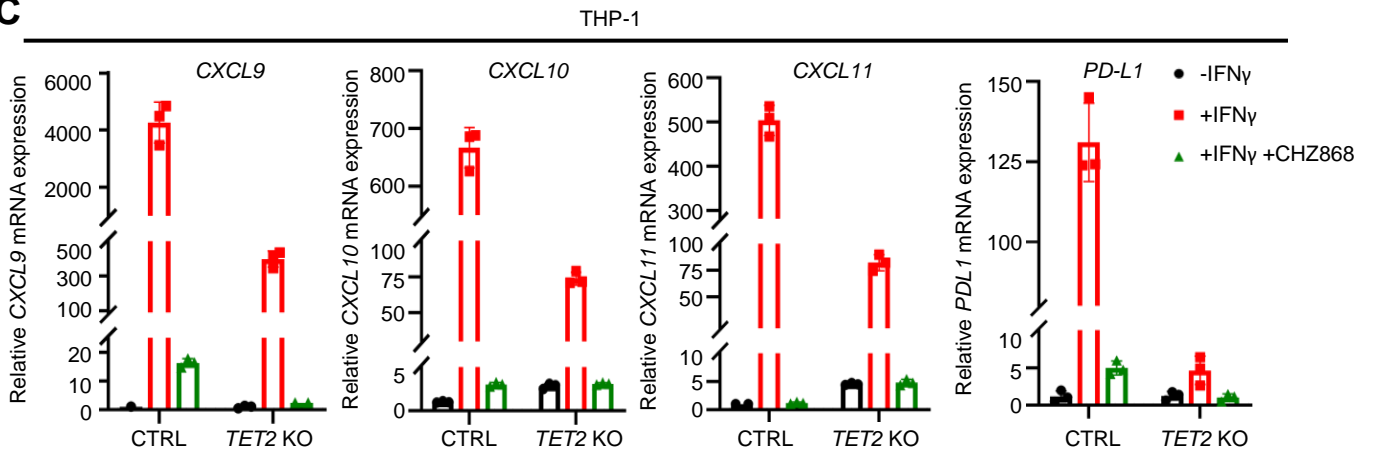
A



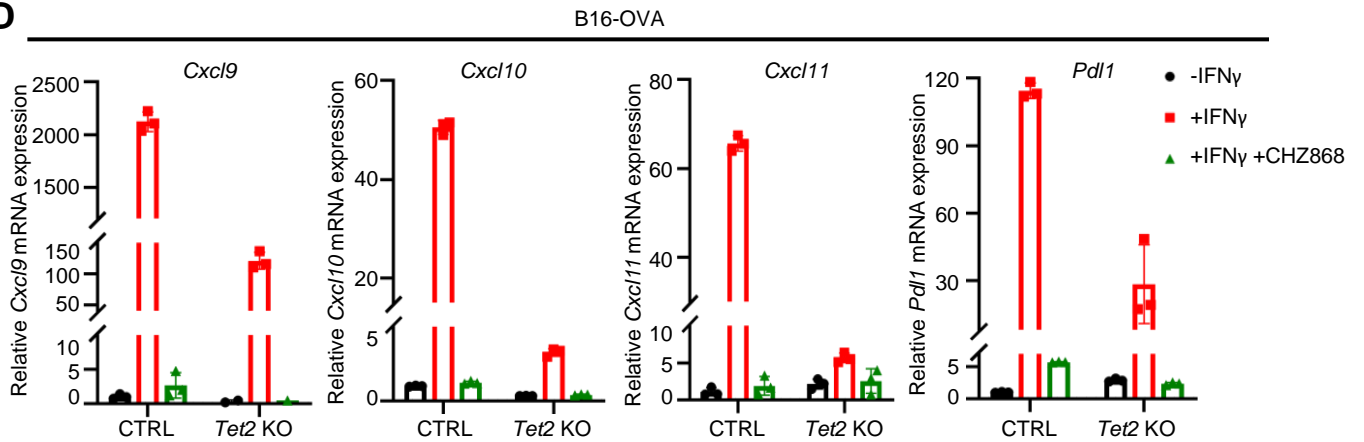
B



C



D



Supplemental Figure 5: TET2 mediates IFN γ -JAK2-STAT1 signaling pathway to activate T_H1-Type chemokines and PD-L1 expression.

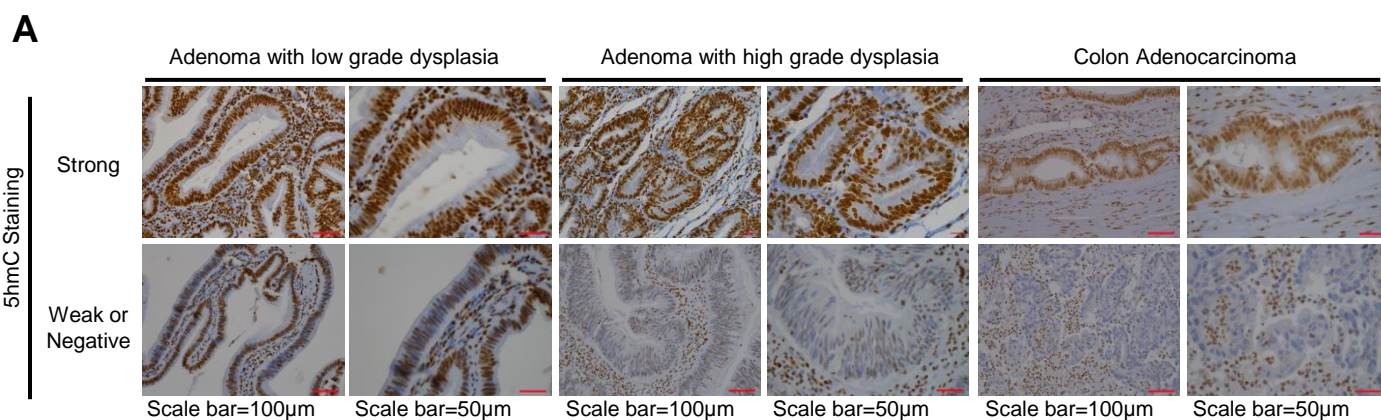
(A): IFN γ promotes Tet2-Stat1 binding. B16-OVA cells were treated with or without IFN γ and the interaction of Tet2 and Stat1 was determined by IP-western blot.

(B): TET2 binds with all 6 STAT family members. Flag-TET2 was transfected into THP-1 cells and followed by Flag-IP. Western-blot was performed by indicated antibodies.

(C): JAK2 inhibitor blocks IFN γ induced T_H1-type chemokines and PD-L1 gene expression in THP-1 cells. Control and *TET2* KO THP-1 cells were treated with IFN γ and JAK2 inhibitor as indicated and mRNA levels of CXCL9/10/11 and PD-L1 were determined by qPCR. Error bars represent \pm SD for triplicate experiments.

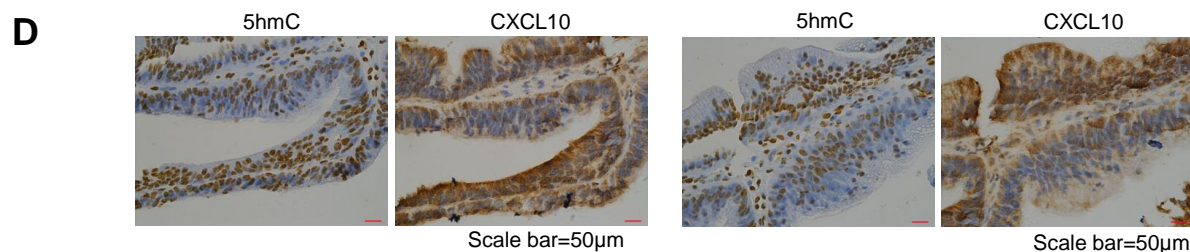
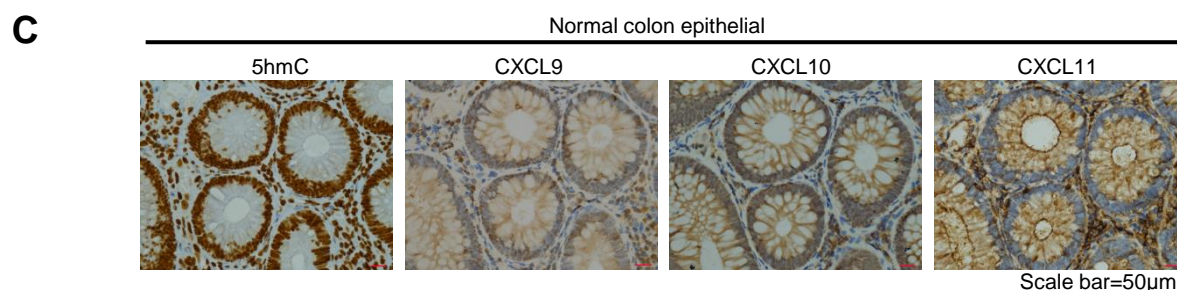
(D): JAK2 inhibitor blocks IFN γ induced T_H1-type chemokines and PD-L1 gene expression in B16-OVA cells. Control and *Tet2* KO B16-OVA cells were treated with IFN γ and JAK2 inhibitor as indicated and mRNA levels of Cxcl9/10/11 and Pdl1 were determined by qPCR. Error bars represent \pm SD for triplicate experiments.

Supplemental Figure 6



B

Colon adenoma	CD3 ⁺ cell number/mm ²	CD8 ⁺ cell number/mm ²	CD56 ⁺ cell number/mm ²
5hmC high group (n=4)	35.41±2.01	11.54±2.7	27.9±4.9
5hmC low group (n=8)	8.01±1.02	2.38±0.48	4.22±0.38
P value	<0.01	<0.01	<0.01



Supplemental Figure 6: 5hmC is lost during colon adenoma progression and correlated with decreased T_H1 type chemokine expression.

(A): 5hmC staining in different stage of colon adenoma. One representative picture of strong or weak 5hmC staining in each stage of colon adenoma is shown.

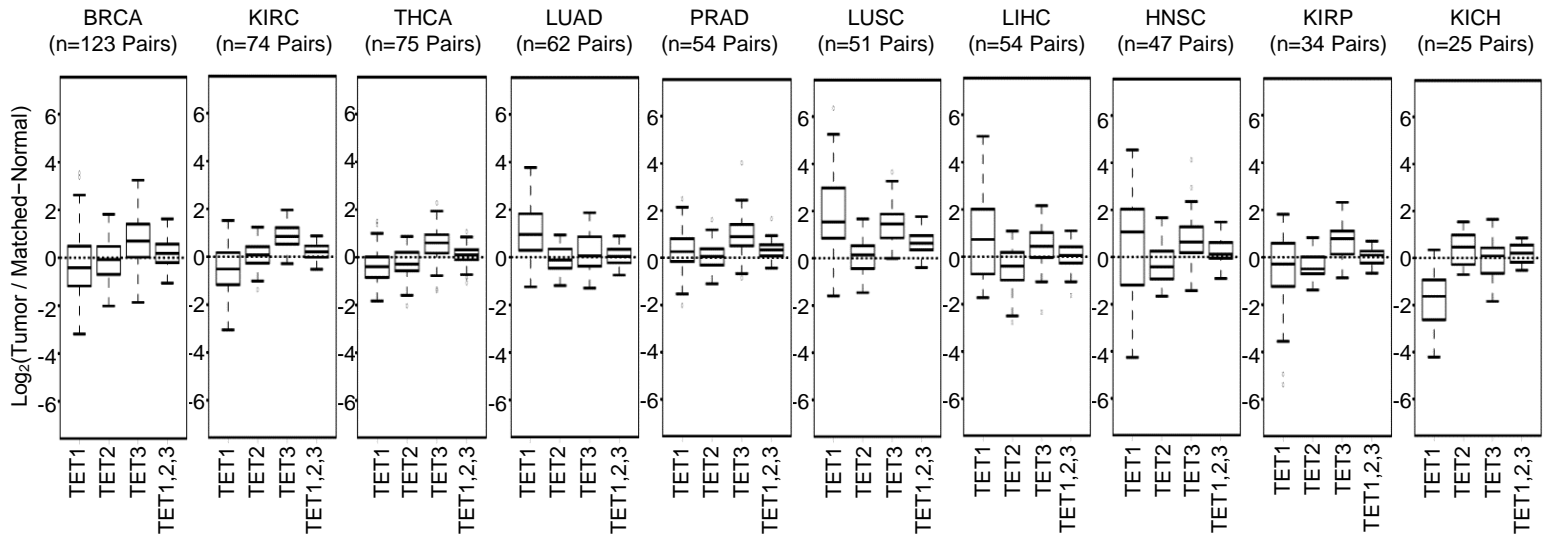
(B): Infiltration lymphocytes in colon adenoma. By using multiple fluorescence staining, infiltration lymphocytes' number was counted in colon adenoma with high or low 5hmC expression. All CD3, CD8, CD56 positive cells were significantly lower in colon adenoma with low 5hmC expression compared with those in colon adenoma with high 5hmC expression.

(C): 5hmC and CXCL9,10,11 staining in normal colon epithelial, scale bar=50µm.

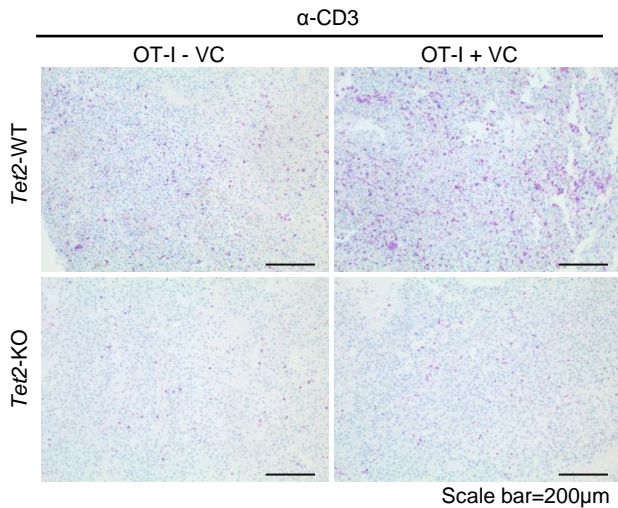
(D): CXCL10 expression level in colon adenoma is tightly correlated with 5hmC level. 5hmC-high areas show strong CXCL10 staining, while 5hmC-decreased areas show weak CXCL10 staining, scale bar=50µm.

Supplemental Figure 7

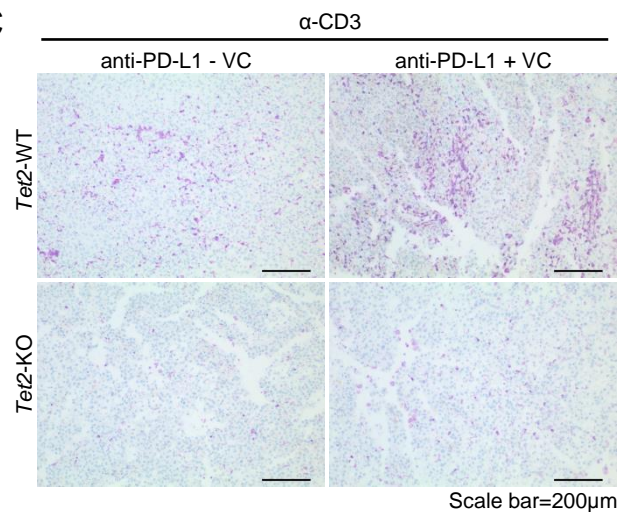
A



B



C



Supplemental Figure 7: Vitamin C stimulates TET activity to enhance tumor-infiltrating lymphocytes.

(A): TET1, TET2 and TET3 mRNA expression in tumor samples and matched normal samples for 10 cancer types from TCGA. TET1,2,3 means sum of TET1/TET2/TET3 mRNA expression. For each box and whisker plot, the ends of the box are the upper (75%) and lower (25%) quartiles, and hence the box spans the interquartile range; the median is marked by the horizontal line inside the box; the whiskers are the two lines outside the box that extend to the highest and lowest observations excluding outliers; while dots outside whiskers are outliers with values larger than 1.5 times of upper quartile or less than 1.5 times of lower quartile.

(B): Vitamin C enhances tumor-infiltrating lymphocytes with adoptive T cell immunotherapy. CD3 immunostaining of *Tet2* WT and KO tumor from Figure 8A treated with adoptive T cell immunotherapy and/or Vitamin C are shown, scale bar=200 μ m.

(C): Vitamin C enhances tumor-infiltrating lymphocytes with anti-PD-L1 immunotherapy. CD3 immunostaining of *Tet2* WT and KO tumors from Figure 9A treated with anti-PD-L1 antibody and/or Vitamin C are shown, scale bar=200 μ m.